Electrostriction of anisotropic tissue

Phillip Prior* and Bradley J. Roth†
Department of Physics, Oakland University, Rochester, Michigan 48309, USA
(Received 25 August 2006; revised manuscript received 13 October 2006; published 5 February 2007)

The electrostrictive effects in anisotropic tissue, such as muscle, are interesting and qualitatively different than in an isotropic material. A striking feature in anisotropic tissue is the presence of a charge distribution, which is absent in isotropic tissue. This charge interacts with the electric field to give rise to body forces that deform the tissue. We develop an electromechanical model to investigate how anisotropic tissue deforms due to an electric field, and find analytical solutions for the pressure and displacement. The distribution of the pressure and displacement are complex and dependent on the boundary conditions. The effects of electrostriction are small, but comparable in size to pressures and displacements in other imaging modalities that utilize similar mechanical effects.

DOI: 10.1103/PhysRevE.75.021903 PACS number(s): 87.19.Rr, 87.10.+e, 87.15.La

I. INTRODUCTION

The interaction of an electric field with matter is a standard topic in introductory physics classes, but often little attention is given to anisotropic materials even though these materials have unique electrostrictive properties [1–3]. Electrostriction is the presence of forces that deform a material, caused by electric fields interacting with charges within the material [4]. This effect is different than piezoelectricity, in which the electric potential gives rise to a mechanical stress in some materials.

There has been a significant body of research on electrostrictive effects in a variety of fields ranging from material science to biology [5–11]. Liquid crystals [5] involve electrostrictive effects and also display anisotropic electrical properties. Polymer field-structured composites have potential applications for fast artificial muscle, while the biological effects of electric fields on membranes has been investigated by various groups [10–15]. Kummrow *et al.* were able to photograph the reversible deformation of giant lipid vesicles in electric field strengths as high as 10^4 V/m [16].

The goal of this paper is to report on the underlying physics of electrostriction in anisotropic media, with an emphasis on the anisotropic electric properties of muscle tissue. We have developed a two-dimensional electromechanical model that combines Navier's equation and the equations of electrostatics. The model predicts the pressure, stress, and strain in response to an electrical field. We present an analytical solution to a relatively simple example, but we believe that our mathematical model will be useful in understanding electrostrictive effects in more complicated systems and situations.

II. METHODS

Consider a cylinder of muscle tissue, which is homogeneous and anisotropic with conductivity σ_x along the muscle fibers (x-direction) and σ_y perpendicular to the fibers (y-direction). The cylinder has radius a, and is uniform along its axis (z-direction). We seek an example that is simple enough to solve analytically, but complicated enough to elucidate the underlying physics. A good compromise is to assume that the potential on the surface of the cylinder is $V_o \cos 3\theta$ (Fig. 1). Outside the cylinder is a homogeneous isotropic fluid, like saline. How will this material deform?

Before attacking the mechanical problem, we must solve the electrostatics problem to determine the current density, $\boldsymbol{J}$, electric field, $\boldsymbol{E}$, and charge density, ρ. The continuity of current ensures that the divergence of the current density equals zero

$$\nabla \cdot \boldsymbol{J} = \sigma_x \frac{\partial E_x}{\partial x} + \sigma_y \frac{\partial E_y}{\partial y} = 0. \tag{1}$$

In the anisotropic tissue ($\sigma_x \neq \sigma_y$), $\nabla \cdot \boldsymbol{J} = 0$ does not imply $\nabla \cdot \boldsymbol{E} = 0$. Gauss's law relates the charge density to the electric field by $\rho = \varepsilon_0 \nabla \cdot \boldsymbol{E}$, where ε_0 is the permittivity of free space [1]. Therefore in anisotropic tissue a charge density exists

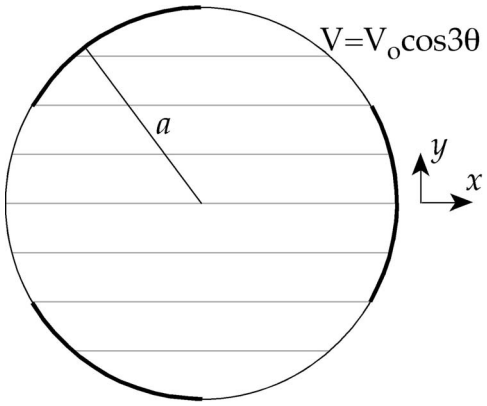

FIG. 1. A schematic diagram depicting a cylinder of anisotropic material. The gray lines indicate the fiber orientation (direction of highest conductivity). The black thick curves on the boundary indicate where the potential is positive. The cylinder is uniform and long in the z-direction.

*Email address: phil.prior@gmail.com
†Corresponding author. FAX: (248) 370-3408. Email address: roth@oakland.edu

that interacts with the electric field to give rise to a force per unit volume, $\boldsymbol{F}$

$$\boldsymbol{F} = \rho \boldsymbol{E} = \varepsilon_0 (\nabla \cdot \boldsymbol{E}) \boldsymbol{E}. \tag{2}$$

This body force contributes to the mechanical stress in the medium, causing it to deform. The situation is completely different in the isotropic fluid, where $\nabla \cdot \boldsymbol{J} = 0$ implies $\nabla \cdot \boldsymbol{E} = 0$ (or equivalently, $\nabla^2 V = 0$, where V is the electric potential); Gauss's law indicates there is no charge density and consequently no body force.

Another way to derive the body force is from the Maxwell stress tensor, T_{ij}. In electrostatics

$$T_{ij} = \varepsilon_0 \left(E_i E_j - \frac{1}{2} \delta_{ij} E^2 \right), \tag{3}$$

where δ_{ij} is the Kronecker delta [1]. In electromagnetic theory, the Maxwell stress tensor plays an important, if somewhat abstract, role related to the momentum flux [1]. In our calculation, its role is very specific: it creates stress in the tissue arising from electrostatic forces acting on charge.

Our mechanical model of tissue allows the material to experience pressure and undergo displacement. The stress tensor, τ_{ij}, is

$$\tau_{ij} = -p \delta_{ij} + 2\mu \varepsilon_{ij} + T_{ij}, \tag{4}$$

where p is the hydrostatic fluid pressure, ε_{ij} is the strain tensor, and μ is the tissue shear modulus. This stress tensor is similar to that in the fluid-fiber-collagen model derived by Chadwick and his colleagues [17–20]. The divergence of Eq. (4) gives Navier's equation that describes the elastic state of the medium in static equilibrium, and says that the sum of the forces is zero. Navier's equation in polar coordinates is [21]

$$-\frac{\partial p}{\partial r} + 2\mu \left(\frac{\partial \varepsilon_{rr}}{\partial r} + \frac{1}{r} \frac{\partial \varepsilon_{r\theta}}{\partial \theta} + \frac{\varepsilon_{rr} - \varepsilon_{\theta\theta}}{r} \right) + F_r = 0, \tag{5}$$

$$-\frac{1}{r} \frac{\partial p}{\partial \theta} + 2\mu \left(\frac{\partial \varepsilon_{r\theta}}{\partial r} + \frac{1}{r} \frac{\partial \varepsilon_{\theta\theta}}{\partial \theta} + \frac{2\varepsilon_{r\theta}}{r} \right) + F_\theta = 0. \tag{6}$$

The displacement of the tissue, $\boldsymbol{u} = (u_r, u_\theta)$, is related to the strain tensor by [21]

$$\varepsilon_{rr} = \frac{\partial u_r}{\partial r}; \quad \varepsilon_{\theta\theta} = \frac{u_r}{r} + \frac{1}{r} \frac{\partial u_\theta}{\partial \theta}; \quad \varepsilon_{r\theta} = \frac{1}{2} \left(\frac{1}{r} \frac{\partial u_r}{\partial \theta} + \frac{\partial u_\theta}{\partial r} - \frac{u_\theta}{r} \right). \tag{7}$$

We assume that the tissue is incompressible ($\nabla \cdot \boldsymbol{u} = 0$), which implies that the displacement can be specified by a stream function ψ, a scalar function whose spatial derivatives give the displacement vector [21]

$$u_r = -\frac{1}{r} \frac{\partial \psi}{\partial \theta}; \quad u_\theta = \frac{\partial \psi}{\partial r}. \tag{8}$$

These relationships allow the solution of Navier's equation to be stated in terms of two scalar functions: the pressure and the stream function. The uniqueness of these solutions will depend on the boundary conditions [22].

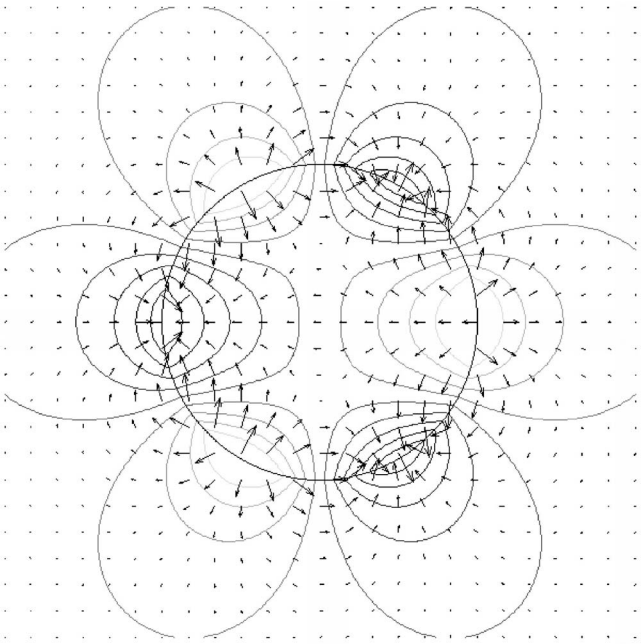

FIG. 2. Electric field (arrows) and potential (contour lines, with light gray lines positive and dark gray lines negative) in and around the cylinder. The material is anisotropic, with $A = 0.69$.

III. RESULTS

The potential inside ($r < a$) and outside ($r > a$) the cylinder is given by

$$V_{\text{out}}(r, \theta) = V_o \left(\frac{a}{r} \right)^3 \cos 3\theta, \tag{9}$$

$$V_{\text{in}}(r, \theta) = V_o \left\{ A \left[\left(\frac{r}{a} \right) - \left(\frac{r}{a} \right)^3 \right] \cos \theta + \left(\frac{r}{a} \right)^3 \cos 3\theta \right\}, \tag{10}$$

where

$$A = 3 \left(\frac{\sigma_x}{\sigma_y} - 1 \right) \Big/ \left(3 \frac{\sigma_x}{\sigma_y} + 1 \right). \tag{11}$$

In the case of isotropic material, $\sigma_x = \sigma_y$ so $A = 0$. For a highly anisotropic material, $\sigma_x \gg \sigma_y$ and A approaches one. A typical value of σ_x / σ_y for muscle is about 4, implying $A \cong 0.69$. The potential and electric field are shown in Fig. 2.

The charge per unit volume inside the anisotropic tissue is

$$\rho_{\text{in}}(r, \theta) = \varepsilon_0 \nabla \cdot \boldsymbol{E} = \frac{V_o \varepsilon_0}{a^2} (8A) \left(\frac{r}{a} \right) \cos \theta, \tag{12}$$

and the charge density outside, in the isotropic fluid, is zero. ρ_{in} is proportional to $x = r \cos \theta$, and is positive on the right side of the cylinder and negative on the left. The charge density and current density are shown in Fig. 3. The charge per unit area, s, on the cylinder surface is

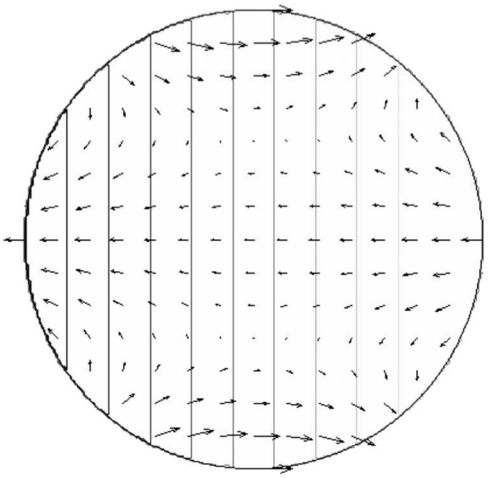

FIG. 3. The current density (arrows) and charge density (contour lines, with light gray lines positive and dark gray lines negative) in the cylinder. The material is anisotropic, with $A=0.69$.

$$s(r,\theta) = \varepsilon_0\left(\frac{\partial V_{\text{in}}}{\partial r} - \frac{\partial V_{\text{out}}}{\partial r}\right)\Bigg|_{r=a} = \varepsilon_0\left(\frac{V_o}{a}\right)[6\cos 3\theta - 2A\cos\theta]. \tag{13}$$

The source of this surface charge is whatever outside agent maintains the potential on the cylinder boundary, such as an electrode or set of electrodes. The surface charge experiences a force analogous to the force attracting the two plates of a capacitor. It is a source of stress in the cylinder even when the material is isotropic.

The body force is given by

$$F_r = \frac{V_o^2\varepsilon_0}{a^3}\left\{4A^2\left[3\left(\frac{r}{a}\right)^3 - \left(\frac{r}{a}\right)\right] - 4\left[A^2\left(\frac{r}{a}\right) + 3A(1-A)\times\left(\frac{r}{a}\right)^3\right]\cos 2\theta - 12A\left(\frac{r}{a}\right)^3\cos 4\theta\right\}, \tag{14}$$

$$F_\theta = \frac{V_o^2\varepsilon_0}{a^3}\left\{\left[4A^2\left(\frac{r}{a}\right) + 4A(3-A)\left(\frac{r}{a}\right)^3\right]\sin 2\theta + 12A\left(\frac{r}{a}\right)^3\sin 4\theta\right\}, \tag{15}$$

and is shown in Fig. 4.

The solution to the mechanical problem depends on the boundary conditions, and we consider two cases: a fixed and a free boundary. A fixed boundary requires the stream function and its radial derivative to be equal to zero at the edge of the cylinder. The pressure and stream functions that satisfy Navier's equation with these boundary conditions are

$$p(r,\theta) = \frac{V_o^2\varepsilon_0}{a^2}\left\{\left[3A^2\left(\frac{r}{a}\right)^4 - 2A^2\left(\frac{r}{a}\right)^2\right] - \left[\left(\frac{5A^2+3A}{2}\right)\left(\frac{r}{a}\right)^2 - \frac{10A^2-6A}{3}\left(\frac{r}{a}\right)^4\right]\cos 2\theta - \left[3A\left(\frac{r}{a}\right)^4\right]\cos 4\theta\right\}, \tag{16}$$

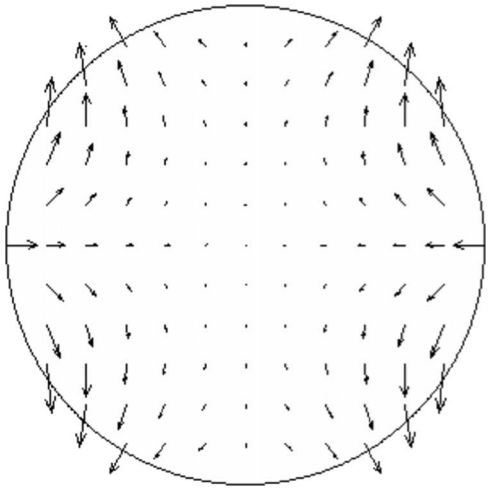

FIG. 4. The body force in the cylinder. The material is anisotropic, with $A=0.69$.

$$\psi(r,\theta) = -\frac{V_o^2\varepsilon_0}{\mu}\left(\frac{A^2+3A}{48}\right)\left[\left(\frac{r}{a}\right)^6 - 2\left(\frac{r}{a}\right)^4 + \left(\frac{r}{a}\right)^2\right]\sin 2\theta. \tag{17}$$

The displacement and pressure are depicted in Fig. 5. The prominent feature is the alternating clockwise and counterclockwise displacement loops in the four quadrants. In an isotropic material, p and ψ both vanish.

A free boundary requires that the components of stress τ_{rr} and $\tau_{r\theta}$ be continuous at $r=a$

$$\tau_{rr} = -p - 2\mu\left(\frac{1}{r}\frac{\partial^2\psi}{\partial r\,\partial\theta} - \frac{1}{r^2}\frac{\partial\psi}{\partial\theta}\right) + T_{rr,i} = T_{rr,o}, \tag{18}$$

$$\tau_{r\theta} = -\mu\left(\frac{1}{r^2}\frac{\partial^2\psi}{\partial\theta^2} - \frac{\partial^2\psi}{\partial r^2} + \frac{1}{r}\frac{\partial\psi}{\partial r}\right) + T_{r\theta,i} = T_{r\theta,o}, \tag{19}$$

where $T_{ij,i}$ and $T_{ij,o}$ are the Maxwell stress tensors inside and outside the cylinder. The solution to Navier's equation with these boundary conditions is

$$p(r,\theta) = \frac{\varepsilon_0 V_o^2}{a^2}\left\{\left[3A^2\left(\frac{r}{a}\right)^4 - 2A^2\left(\frac{r}{a}\right)^2\right] + \left[\left(\frac{10A^2}{3} - 2A\right)\times\left(\frac{r}{a}\right)^4 - \left(\frac{5A^2}{2} - \frac{3A}{2}\right)\left(\frac{r}{a}\right)^2\right]\cos 2\theta - 9\left(\frac{r}{a}\right)^6\cos 6\theta\right\}, \tag{20}$$

$$\psi(r,\theta) = \frac{\varepsilon_0 V_o^2}{\mu}\left\{\left[\left(\frac{A}{16} + \frac{A^2}{48}\right)\left(\frac{r}{a}\right)^2 + \left(\frac{A^2}{24} - \frac{A}{8}\right)\left(\frac{r}{a}\right)^4 - \left(\frac{A}{16} + \frac{A^2}{48}\right)\left(\frac{r}{a}\right)^6\right]\sin 2\theta + \left[\frac{A}{8}\left(\frac{r}{a}\right)^4 - \frac{3A}{20}\left(\frac{r}{a}\right)^6\right]\sin 4\theta - \left[\frac{3}{10}\left(\frac{r}{a}\right)^6 - \frac{9}{28}\left(\frac{r}{a}\right)^8\right]\sin 6\theta\right\}. \tag{21}$$

The displacement of anisotropic tissue for a free boundary

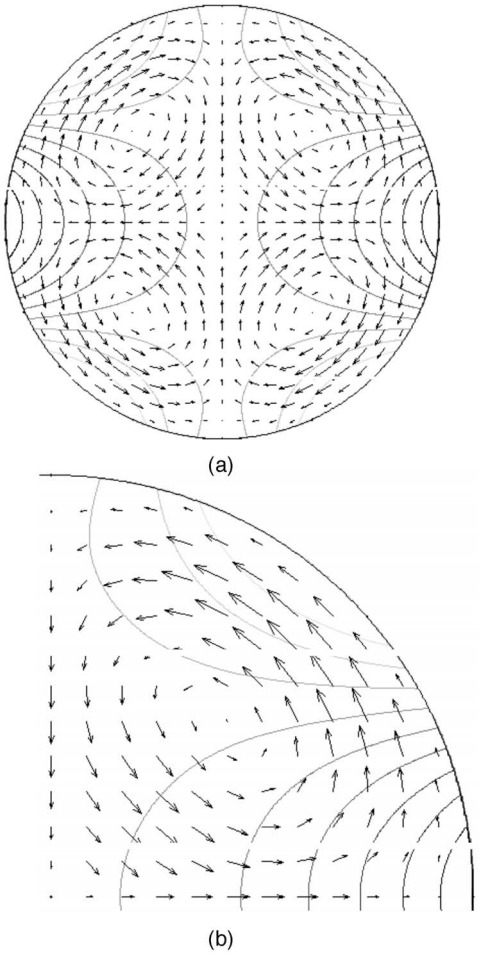

FIG. 5. The displacement (arrows) and pressure (contour lines, with light gray lines positive and dark gray lines negative) for a fixed boundary. The material is anisotropic, with $A=0.69$. (a) The entire cylinder cross section and (b) one quadrant is expanded to show the detail.

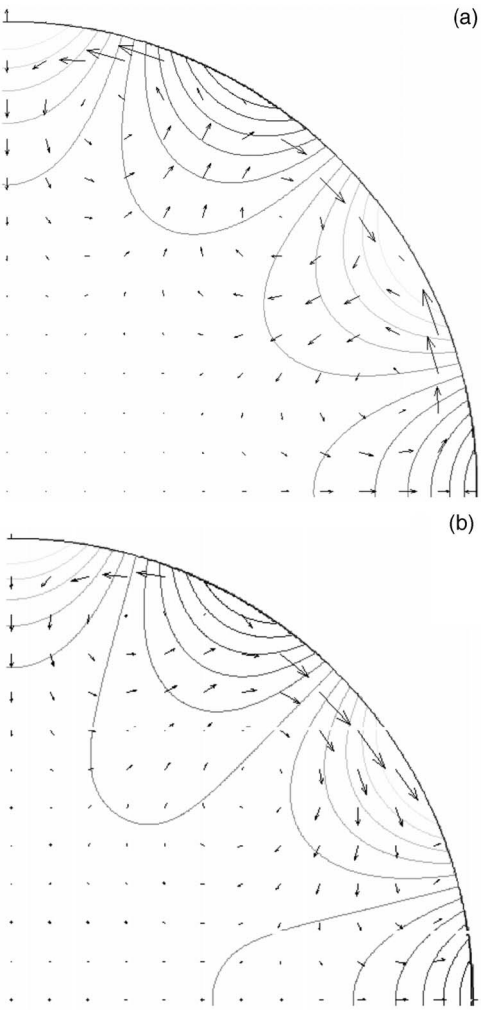

FIG. 6. The displacement (arrows) and pressure (contour lines, with light gray lines positive and dark gray lines negative) for a free boundary. Only one quadrant is shown. (a) The material is isotropic and (b) the material is anisotropic with $A=0.69$.

retains a mixture of clockwise and counterclockwise displacement loops but is more complicated than for a fixed boundary. Figure 6(a) shows the pressure and displacement of isotropic tissue. The surface charge interacts with the electric field to give rise to nonzero pressure and displacement, which vanish for a fixed boundary. The displacement and pressure for anisotropic tissue are shown in Fig. 6(b).

IV. DISCUSSION

We have developed an electromechanical model for calculating the electrostrictive deformation of anisotropic tissue and used this model to calculate the pressure and displacement in a cylinder of muscle. The distribution of displacement and pressure is complex and depends on the boundary conditions. An electric field induces a strain but, unlike piezoelectricity, a strain does not induce an electric field. This strain has nothing to do with a muscle's ability to contract via the interaction of actin and myosin fibers, and it would occur in any anisotropic medium, biological or not.

Our mechanical model is motivated by the fluid-fiber-collagen model of cardiac tissue [17–19]. In our calculation we make several assumptions.

(1) Strains are small enough for a linear model of elasticity.
(2) The tissue is in quasistatic mechanical equilibrium.
(3) The tissue is incompressible.
(4) The fibers are straight and parallel to one another.
(5) Electrical conductivities are anisotropic while the mechanical properties (shear modulus) are isotropic.

Although some of these assumptions are probably accurate (e.g., quasistatic mechanical equilibrium, incompressible medium, and small strains), the simple fiber geometry and isotropic mechanical properties are a significant simplification of the structure of a real muscle. We assumed an isotropic mechanical model because we desired an analytical solution of the problem to best illustrate the underlying physics, and anisotropic mechanical problems are notoriously difficult to solve analytically. Our model yields solutions for the pres-

sure and displacement. The analytical expressions demonstrate at a glance how electrostriction depends on the parameters of the model. Solutions to more realistic situations will require the adoption of numerical methods. Our analytic solutions will be useful in validating such numerical solutions.

Electrostrictive effects are small. Pressures are on the order of $\varepsilon_0 E^2$, where E is the electric field (V/m) and $\varepsilon_0 = 8.85 \times 10^{-12}$ Pa/(V/m)^2 [1]. Displacements caused by electrostriction are on the order of $(\varepsilon_0 E^2 a)/\mu$ where a is the length characteristic of the particular problem (m) and μ is the shear modulus of the tissue (Pa). Because ε_0 is small, E must be large before the pressure and displacement are significant. What biomedical applications require large electric fields? Defibrillation, electroporation, tissue ablation, electroconvulsive therapy, and potentially artificial muscle all use large fields. Transthoracic defibrillation often produces electric field strengths of up to 3000 V/m [23–25], and the electric field near the electrode tip of an implantable defibrillator is even higher, probably on the order of 10^4 V/m. Electric fields of this magnitude may produce a measurable deformation due to electrostrictive effects.

The maximum magnitudes of the displacement and pressure in our model with a fixed boundary are $|p(r,\theta)| = 5.0 \times 10^{-4}$ Pa, $|\boldsymbol{u}(r,\theta)|_{\max} = 1.3 \times 10^{-12}$ m, and with a free boundary are $|p(r,\theta)| = 12 \times 10^{-4}$ Pa, $|\boldsymbol{u}(r,\theta)|_{\max} = 1.1 \times 10^{-10}$ m. These calculations were done assuming a potential of 20 V over $a = 0.005$ m, $\sigma_x/\sigma_y = 4$, and a shear modulus, μ, of 5000 Pa [19]. The use of a 40 V/cm voltage gradient is consistent with electric fields used in transthoracic defibrillation studies [23]. The displacements and pressures are small but measurable. Yimnirun *et al.* use a single beam interferometer to measure 10^{-4} Å displacements [26]. Xu and He indicate in mPa pressures are measurable with current acoustic detectors [27].

The magnitudes of the displacement and pressure are proportional to the square of the applied voltage. This nonlinearity arises because both the electric field and the charge are proportional to the voltage, and their product is the body force. If the voltage is alternating, proportional to $\cos(\omega t)$, then the pressure and displacement will be proportional to $\cos^2(\omega t) = [1 + \cos(2\omega t)]/2$. Thus an ac voltage will cause a dc pressure and an ac pressure at twice the applied frequency. If the frequency is too large, our assumption of quasistationarity will no longer hold. Electrically, quasistationarity means that all currents and fields behave as if they are static, implying that we can ignore electromagnetic radiation, Faraday induction, and capacitive effects [28]. Mechanically, quasistationarity means that we can ignore acoustic waves.

Electrostrictive effects are comparable to similar mechanical effects in imaging modalities such as magnetoacoustic imaging, in which one measures ultrasonic vibration to image the electric current in biological tissue [29–32]. A similar modality, magnetoacoustic tomography with magnetic induction (MAT-MI), is a combination of magnetoacoustic imaging and magnetic induction that combines pulsed magnetic stimulation with sonography to noninvasively image the electrical impedance of samples [27,33]. Magnetic resonance techniques have been used to measure the elastic properties of tissue. Dubbed magnetic resonance elastography (MRE), this technique utilizes a phase contrast method to visualize propagating strain waves in material [34–36]. Lorentz force imaging maps the electric current distribution in biological material. An ultrasonic wave causes ions to move in the tissue, and in the presence of a dc magnetic field, these ions experience a Lorentz force which gives rise to a local current density proportional to the electrical conductivity [37–40]. All of these imaging techniques illustrate the ability of many experimentalists to measure small effects, and for each modality electrostrictive effects may contribute to the measured signal.

ACKNOWLEDGMENTS

We thank Steffan Puwal and Michelle Fritz for their comments and advice.

[1] D. J. Griffiths, *Introduction to Electrodynamics*, 3rd ed. (Prentice-Hall, Englewood Cliffs, NJ, 1999).
[2] J. D. Jackson, *Classical Electrodynamics*, 3rd ed. (Wiley, New York, 1999).
[3] E. M. Lifshitz, L. D. Landau, and L. P. Pitaevskii, *Electrodynamics of Continuous Media*, 2nd ed. (Pergamon, New York, 1984), Vol. 8.
[4] W. G. Cady, *Piezoelectricity* (Dover, New York, 1964).
[5] P. G. de Gennes and J. Prost, *The Physics of Liquid Crystals*, 2nd ed. (Oxford University Press, Oxford, 1993).
[6] J. E. Martin and R. A. Anderson, J. Chem. Phys. **111**, 4273 (1999).
[7] Q. M. Zhang, J. Su, C. H. Kim, R. Ting, and R. Capps, J. Appl. Phys. **81**, 2770 (1997).
[8] Q. M. Zhang, V. Bharti, and X. Zhao, Science **280**, 2101 (1998).
[9] P. Kietis, M. Vengris, and L. Valkunas, Biophys. J. **80**, 1631 (2001).
[10] H. G. L. Coster, Aust. J. Phys. **52**, 117 (1999).
[11] H. G. L. Coster and U. Zimmermann, J. Membr. Biol. **22**, 73 (1975).
[12] U. Zimmermann, F. Beckers, and H. G. L. Coster, Biochim. Biophys. Acta **464**, 399 (1977).
[13] H. G. L. Coster, D. R. Laver, and J. R. Smith, in *Biochemistry*, edited by H. Keyzer and F. Gutmann (Plenum, New York, 1980), pp. 331–352.
[14] H. G. L. Coster, *in Electropharmacology*, edited by G. M. Eckert *et al.* (CRC Press, Boca Raton, FL, 1990), pp. 139–158.
[15] H. G. L. Coster and T. C. Chilcott, Bioelectrochemistry **56**, 141 (2002).
[16] M. Kummrow and W. Helfrich, Phys. Rev. A **44**, 8356 (1991).
[17] R. S. Chadwick, Biophys. J. **39**, 279 (1982).
[18] J. Ohayon and R. S. Chadwick, Biophys. J. **54**, 1077 (1988).
[19] R. S. Chadwick, J. Ohayon, and M. Lewkowicz, Proc. Natl.

Acad. Sci. U.S.A. **86**, 2996 (1989).
[20] D. C. Latimer, B. J. Roth, and K. K. Parker, Tissue Eng. **9**, 283 (2003).
[21] A. E. H. Love, *A Treatise on the Mathematical Theory of Elasticity* (Dover, New York, 1944).
[22] A. Aldroubi and R. S. Chadwick, Math. Biosci. **99**, 195 (1990).
[23] J. T. Niemann, R. G. Walker, and J. P. Rosborough, Acad. Emerg. Med. **12**, 99 (2005).
[24] H. G. L. Coster, J. Biol. Phys. **29**, 363 (2003).
[25] J. M. Crowley, Biophys. J. **13**, 771 (1973).
[26] R. Yimnirun, P. J. Moses, R. J. Meyer, Jr., and R. E. Newnham, Meas. Sci. Technol. **14**, 766 (2003).
[27] Y. Xu and B. He, Phys. Med. Biol. **50**, 5175 (2005).
[28] R. Plonsey, *Bioelectric Phenomena* (McGraw-Hill, New York, 1969).
[29] B. J. Roth, P. J. Basser, and J. P. Wikswo, Jr., IEEE Trans. Biomed. Eng. **41**, 723 (1994).
[30] B. C. Towe and M. R. Islam, IEEE Trans. Biomed. Eng. **35**, 892 (1988).
[31] B. C. Towe, IEEE Trans. Biomed. Eng. **44**, 455 (1997).
[32] M. R. Islam and B. C. Towe, IEEE Trans. Med. Imaging **7**, 386 (1988).
[33] X. Li, Y. Xu, and B. He, J. Appl. Phys. **99**, 066112 (2006).
[34] M. Suga, T. Matsuda, K. Minato, O. Oshiro, K. Chichara, J. Okamoto, O. Takizawa, M. Komori, and T. Takahashi, IEEE Trans. Biomed. Eng. **50**, 933 (2001).
[35] I. Sack, A. Samani, D. Plewes, and J. Braun, Magn. Reson. Med. **11**, 587 (2003).
[36] M. A. Dresner, G. H. Rose, P. J. Rossman, R. Muthupillai, A. Manduca, and R. L. Ehman, J. Magn. Reson Imaging **13**, 269 (2001).
[37] A. Montalibet, J. Jossinet, and A. Matias, Ultrason. Imaging **23**, 117 (2001).
[38] A. Montalibet, J. Jossinet, A. Matias, and D. Cathignol, Med. Biol. Eng. Comput. **39**, 15 (2001).
[39] H. Wen, Ultrason. Imaging **21**, 186 (1999).
[40] B. J. Roth and J. P. Wikswo, Jr., IEEE Trans. Biomed. Eng. **45**, 1294 (1998).